Supporting Information

Bacterial Detection and Elimination Using a Dual-Functional Porphyrin-Based Porous Organic Polymer with Peroxidase-Like and High Near-Infrared-Light-Enhanced Antibacterial Activity

Dekang Li,[a] Yishan Fang,[b] and Xiaomei Zhang*[a]

[a] School of Chemistry and Chemical Engineering, Shandong University, Jinan, Shandong 250100, China

[b] School of Food Science and Engineering, Qilu University of Technology, Shandong Academy of Sciences, Jinan 250353, China

Corresponding Author

* E-mail: zhangxiaomei@sdu.edu.cn (X. Zhang)

S1. Instrumentation and Methods. Fourier transform infrared spectra (FT-IR) were obtained in KBr pellets with 2 cm^{-1} resolution on an ALPHA-T spectrometer (Bruker, Germany). Solid-state ^{13}C CP/MAS NMR experiments were performed on a Bruker AVANCE III 600 (Germany) spectrometer using a 4 mm MAS probe and a spinning rate of 12 kHz. The Hitachi S-4800 (Japan) scanning electron microscopy (SEM) was used to obtain SEM images. The UV-vis diffuse reflectance spectra were characterized by a Shimadzu UV-3600 UV-vis-near-IR spectrophotometer (Shimadzu Co., Japan). To prevent charging effects and improve image clarity, Au (1-2 nm) was sputtered onto the grids. N_2 adsorption-desorption (Tristar II 3020, Micromeritics, USA) was measured at 77.3 K and the surface area of $FePPOP_{BPBF}$ was calculated by both the Brunauer-Emmett-Teller (BET) and Langmuir methods. Thermogravimetric measurements were performed on a Mettler Toledo TGA/SDTA 851^o under N_2 (heated to 600 ^oC, 10 $^oC \cdot min^{-1}$). Elemental analyses were performed by Vavio E1 III (Elementar, Germany). The Fe and Au contents of the PPOPs samples were detected by inductively coupled plasma atomic emission spectroscopic (ICP-AES) analysis with an IRIS Intrepid II XRP instrument. The colorimetric immunoassay measurements were carried out on EnSpire multimode plate readers (PerkinElmer). The photothermal study was done by using a 808 nm continuous-wave semiconductor laser (FC-808-2000-MM). Photothermal effects were measured by a mini dual temperature thermometer (UT320A) and the temperature change was recorded once per 20 s.

S2. Preparation of $FePPOP_{BFPB}$ and $Au@FePPOP_{BFPB}$. $FePPOP_{BFPB}$ was synthesized through a simple hydrothermal strategy. Freshly distilled pyrrole (10 μL, 0.12 mmol) and BFPP (100 mg, 0.18 mmol), $FeCl_3 \cdot 6H_2O$ (21.9 mg, 0.081 mmol) were dispersed in 100 mL propionic acid and the reaction system was stirred under N_2 at 25 °C for 4 h. Then the solution was transferred into a tetrafluoroethylene-lined autoclave and heated at 180 °C for 72 h. After cooling to room temperature, the dark brown precipitate was filtered and the precipitate was repeatedly washed with DMF, ultrapure water, and methanol until the filtrate became colorless. Finally, the resultant $FePPOP_{BFPB}$ nanoparticles were s dried in a vacuum at 80 °C for 24 h. $FePPOP_{BFPB}$ was obtained as a brown powder with a yield of 60 %. The Elemental analysis value obtained by combustion was C, 68.21 %; H, 4.881 %; N, 5.4 %. The calculated theoretical formula of $FePPOP_{BFPB}$ was C, 71.14 %; H, 5.37 %; N, 10.29 %. ICP-AES analysis showed that the Fe content was 0.386 %.

To facilitate the conjugation of the bs-4582R with $FePPOP_{BFPB}$, a small amount of Au was photodeposited on the surface of $FePPOP_{BFPB}$. Briefly, 30.5 mg of $FePPOP_{BFPB}$ and NaOH (0.2 M, 1 mL) were mixed with 20 mL ethanol. After sonication for 3 minutes, 2 mL $HAuCl_4$ (0.8 wt %) was slowly added to the solution. Then, the mixture was irradiated with a 500 W xenon lamp, and stirred for 12 h until the solution turned reddish-brown. The precipitate was washed with water and ethanol at least three times to remove free nanoparticles for further investigation. After vacuum drying at 80 °C for 24 h, 37.7 mg of $Au@FePPOP_{BFPB}$ was obtained as a brown powder. ICP-AES analysis showed that the Fe and Au contents were 0.34 % and 5.35 %, respectively.

S3. Peroxidase Activity Measurements, Stability Test and Kinetic Analysis of $FePPOP_{BFPB}$. The catalytic activity experiments were done by monitoring the absorbance change of peroxidase-like $FePPOP_{BFPB}$ with 3,3′,5,5′-tetramethylbenzidine (TMB) at 25 °C for 3 min. The final concentrations of H_2O_2, TMB, and $FePPOP_{BFPB}$ were 40 mM, 0.1 mM, and 10 μg·mL^{-1}, respectively. The buffer solution (pH=3.8) contained NaOAc and HOAc. To obtain optimum conditions for catalytic activity, the pH values (1.70-11.10), temperature (5-65 °C), and H_2O_2 concentrations (0.5-80 mM) were carried out under the same conditions. In addition, five cycle tests was used to verify the stability of $FePPOP_{BFPB}$. The other experimental conditions were same as the peroxidase activity measurements. The kinetic analyses were measured by using $FePPOP_{BFPB}$ (10 μg·mL^{-1}) with (i) a fixed amount of H_2O_2 (40 mM) and different amounts of TMB (0-0.2 mM) solution, and (ii) a fixed amount of TMB (0.1 mM) and different amounts of H_2O_2 (0-30 mM). All reactions were monitored by measuring the absorbance at 652 nm using a Hitachi U-400 UV-vis spectrophotometer.

S4. Preparation of Ab_2@Au@$FePPOP_{BFPB}$. The Ab_2@Au@$FePPOP_{BFPB}$ was prepared via the bioconjugation of Au@$FePPOP_{BFPB}$ with bs-4582R antibody, denoted as Ab_2 according to the previous literature. In detail, 10 mg of the Au@$FePPOP_{BFPB}$ hybrid were dispersed in 9 mL of PBS (0.01 M, pH=7.4) with Ab_2 (25 μg/mL, 2 mL) and ultrasonically vibrated for 15 s. The resulting solution was incubated at 4 °C with slight shaking for 24 h. During this process, Ab_2 were covalently conjugated with Au@$FePPOP_{BFPB}$ on the basis of the interaction between cysteine/$NH3^+$-lysine residues of the Ab_2 and Au.[1] Then, the BSA blocking buffer (5 wt %, 5 mL, diluted in

PBS, pH=7.40) was added and incubated at 4 °C for 12 h to block the possible residual sites on Au@FePPOP$_{BFPB}$. After being purified and collected by centrifuging, the resulting Ab$_2$@Au@FePPOP$_{BFPB}$ conjugates were dispersed in 9 mL of PBS and stored at 4 °C for further use.

Confirming the Bioconjugation of Antibodies to Au@FePPOP$_{BFPB}$

As can be seen in Figure S1, two characteristic peaks at 1672 and 1533 cm^{-1} were observed in the FT-IR spectra of pure antibody (bs-4582R, Ab$_2$) (curve 'a'), which corresponded to the amide I and II groups of Ab$_2$ proteins. When Ab$_2$ were immobilized onto the Au@FePPOP$_{BFPB}$, the absorption bands for amide I and amide II could also be obviously observed (curve 'b'). These results revealed that Ab$_2$ could be conjugated onto the Au@FePPOP$_{BFPB}$ through the formation of the Au-S bond or Au-NH bond due to the interaction between cysteine or NH3$^+$-lysine residues of Ab$_2$ and the Au@FePPOP$_{BFPB}$.

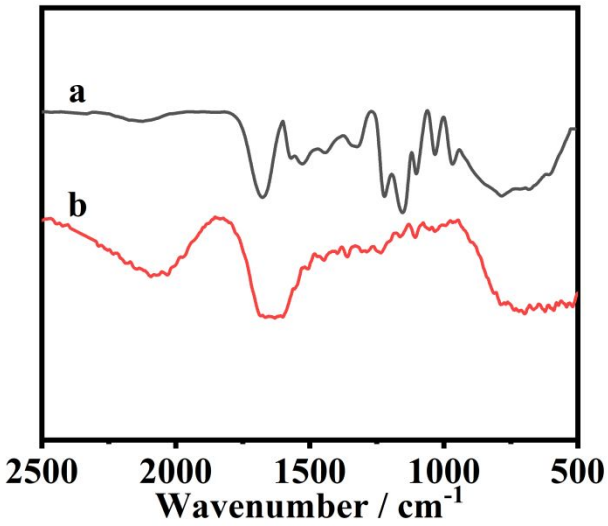

Figure S1. FT-IR spectra of (a) antibody (bs-4582R, Ab$_2$) and (b) Ab$_2$@Au@FePPOP$_{BFPB}$.

Calculating the Conjugation Amount and the Conjugation Efficiency of Antibody (bs-4582R, Ab_2) to $Au@FePPOP_{BFPB}$

To calculate the conjugation amount and the conjugation efficiency of antibody (bs-4582R, Ab_2) to $Au@FePPOP_{BFPB}$, the standard concentration curve of antibodies was monitored, firstly, Figure S2.

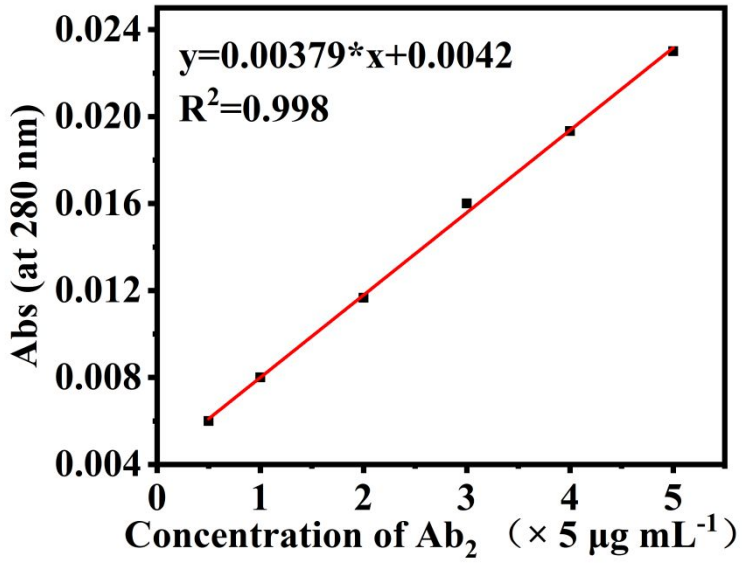

Figure S2. The standard concentration curve of antibody (bs-4582R, Ab_2).

Then, 10 mg of the $Au@FePPOP_{BFPB}$ hybrid were dispersed in 9 mL of PBS (0.01 M, pH=7.4) with Ab_2 (25 μg/mL, 2 mL) and ultrasonically vibrated for 15 s. The resulting solution was incubated at 4 °C with slight shaking for 24 h. Then, $Ab_2@Au@FePPOP_{BFPB}$ was separated by centrifuging. The amount of Ab_2 loaded on $Au@FePPOP_{BFPB}$ (Q_e, μg mg^{-1}) can be calculated by the concentration change of Ab_2 solution as monitored by the UV-Vis spectroscopy by using the Eq. 1.

$$Q_e = \frac{(C_0 - C_e)V}{m} \quad \text{(Eq. 1)}$$

where C_0 and C_e (μg mL^{-1}) are the initial and final concentrations of Ab_2, respectively, V (mL) is the volume of the Ab_2 solution, and m (mg) is the weight of Au@$FePPOP_{BFPB}$. The conjugation efficiency of antibody (bs-4582R, Ab_2) to Au@$FePPOP_{BFPB}$ can be calculated by the following:

$$\eta = \frac{C_0 - C_e}{C_0} \times 100\ \% \quad \text{(Eq. 2)}$$

The specific calculation process is as follows:

$$C_e = \frac{0.0056 - 0.0042}{0.00379} \times 5\ \mu g\ mL^{-1} = 1.85\ \mu g\ mL^{-1}$$

$$Q_e = \frac{(4.545 - 1.85) \times 11}{10} = 2.965\ \mu g\ mg^{-1}$$

$$\eta = \frac{4.545 - 1.85}{4.545} \times 100\ \% = 59.3\%$$

The result indicated that the conjugation amount and the conjugation efficiency of antibody (bs-4582R, Ab_2) to Au@$FePPOP_{BFPB}$ was 2.965 μg mL^{-1} and 59.3 % respectively.

S5. Calculation of the Photothermal Conversion Efficiency (η) of $FePPOP_{BFPB}$. Photothermal properties of the $FePPOP_{BFPB}$ were measured according to the previous reports. The photothermal conversion efficiency (η) was calculated as follows: 1 mL of the $FePPOP_{BFPB}$ aqueous dispersion of different concentrations (0, 62.5, 125, 250, 500 and 1000 ppm) were exposed to 808 nm NIR laser for 850 s, and then the laser was shut off to let the solution cool to room temperature. Photothermal effects were measured by a mini dual temperature thermometer (UT320A). Then, the η value was calculated according to Eq. 3.

$$\eta = \frac{hA(T_{max} - T_{amb}) - Q_0}{I(1 - 10^{-A_\lambda})} \quad \text{(Eq. 3)}$$

Here, h is the heat transfer coefficient, A is the surface area of the container, T_{max} is the maximum system temperature, T_{amb} is the ambient surrounding temperature. Q_0 is the baseline energy input by the solvent and sample container without the $FePPOP_{BFPB}$. I is the laser power and A_λ is the absorbance at 808 nm. The lumped value of hA was determined by measuring the drop rate of temperature after removing the light source and the value of hA is derived according to Equations 4 and 5.

$$\tau_s = \frac{m_D - C_D}{hA} \qquad \text{(Eq. 4)}$$

$$\theta = \frac{T_{amb} - T}{T_{amb} - T_{max}} \qquad \text{(Eq. 5)}$$

where τ_s is the sample system time constant, m_D and C_D are the mass (1 g) and heat capacity (4.2 J g^{-1} k^{-1}) of deionized water used as solvent, respectively. The time constant was τ_s = 319.67 s based on the linear fit from the cooling period after 850 s vs. -lnθ as shown in Figure S2D. The heat energy (Q_0) of the sample container and solvent without $FePPOP_{BFPB}$ was measured independently using Eq. 6.

$$Q_0 = (hA)'(T_{max} - T_{amb}) \qquad \text{(Eq. 6)}$$

Accordingly, the photothermal conversion efficiency calculated by Eq. 1-4 was η = 35.6 %.

S6. Recycling Experiments of $FePPOP_{BFPB}$ for Catalyzed Oxidation of TMB. Primarily, 0.1 mg of material is dispersed in 8 ml of ultrapure water. Then, H_2O_2 (1mL，400 mM), TMB (1mL, 1 mM) was joined into the above system. The final concentrations of H_2O_2, TMB, and $FePPOP_{BFPB}$ were 40 mM, 0.1 mM, and 10 μg·mL^{-1}, respectively. The reaction of system was operated in the dark for 3 minutes at 25 ^oC.The supernatant was separated by centrifugating and monitored by measuring the

absorbance at 652 nm. The centrifuged solid catalyst was washed with water and reused without further process.

S7. Calculation of the Kinetic Parameters of $FePPOP_{BFPB}$. The steady-state kinetic parameters for $FePPOP_{BFPB}$ were measured according to the previous reports.[2] Absorbance data were back-calculated to concentration by the Beer-Lambert Law using a molar absorption coefficient for TMB derived oxidation products ($\varepsilon_{652\ nm}$ =39 mM^{-1} cm^{-1}). Apparent steady-state reaction rates at different concentrations of substrate were obtained by time-scanning curves with a UV-vis spectrophotometer at the wavelength of 652 nm. The initial velocities were fit with the substrate concentrations using typical Michaelis-Menten equation:

$$V = \frac{V_{max}[S]}{K_m + [S]} \qquad \text{(Eq. 7)}$$

where [S] is the concentration of the substrate, V is the initial velocity, V_{max} is the maximal velocity, and K_m is the Michaelis constant. Using Lineweaver-Burk equation, which was describe as $1/V = (K_m/V_{max})(1/[S]) + 1/V_{max}$ (Eq. 8), double-reciprocal model derived from the Michaelis-Menten equation, K_m and V_{max} of $FePPOP_{BFPB}$ with the substrate H_2O_2 and TMB were obtained.

Related Figures

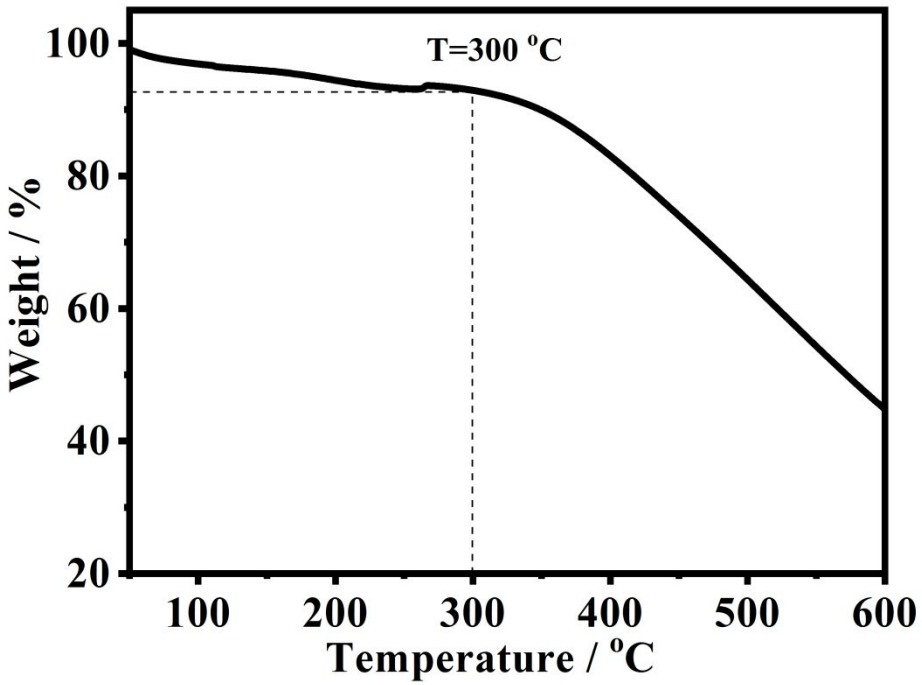

Figure S3. Thermogravimetric analysis (TGA) data of $FePPOP_{BFPB}$.

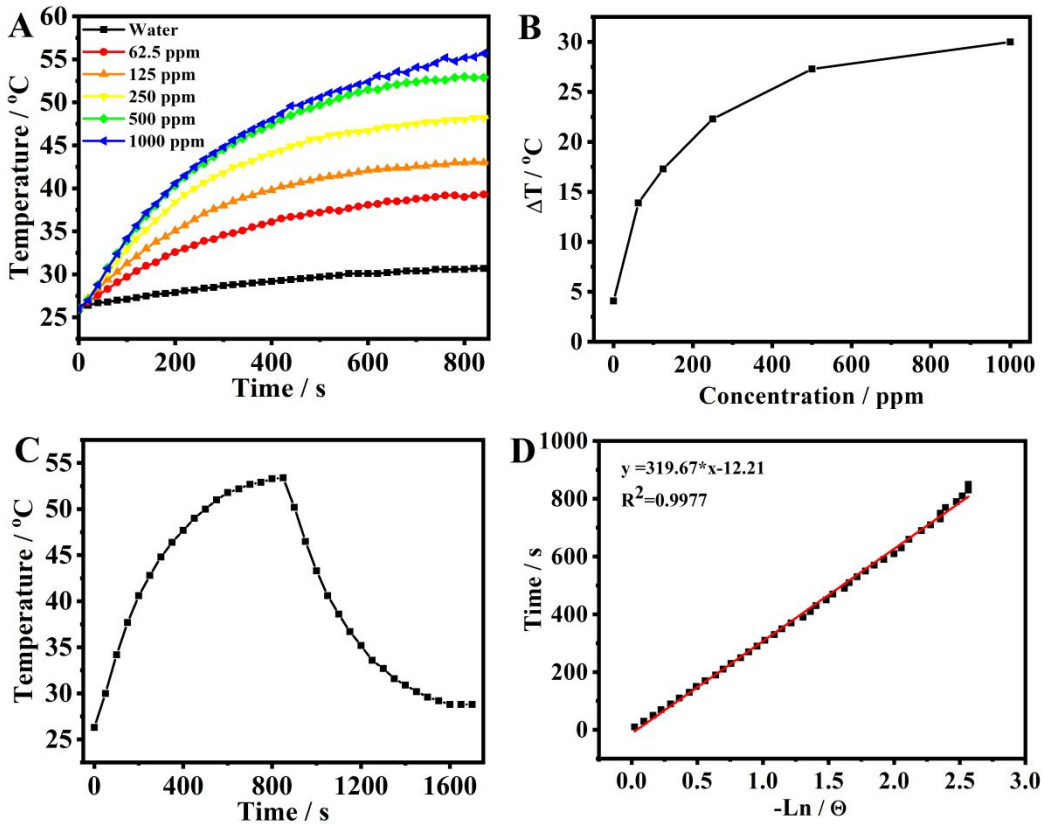

Figure S4. (A) Temperature changes based on the $FePPOP_{BFPB}$ concentration under 808 nm laser irradiation. (B) Temperature increment over a period of exposure to the 808 nm laser (1.2 W/cm^2) at various $FePPOP_{BFPB}$ concentrations. (C) The photothermal effect of $FePPOP_{BFPB}$ aqueous solution under 808 nm NIR laser irradiation for 850 s and then turn off the NIR laser for 850 s. An 808 nm laser with a power density of 1.2 W/cm^2 was used. The concentration of $FePPOP_{BFPB}$ in water is 500 ppm (500 μg/mL). (D) The time constant (τ_s) for heat transfer from the system was calculated to be 319.67 s by applying the linear time data from the cooling period of (C) versus the negative natural logarithm of the driving force temperature. The concentration of $FePPOP_{BFPB}$ in water is 500 ppm (500 μg/mL).

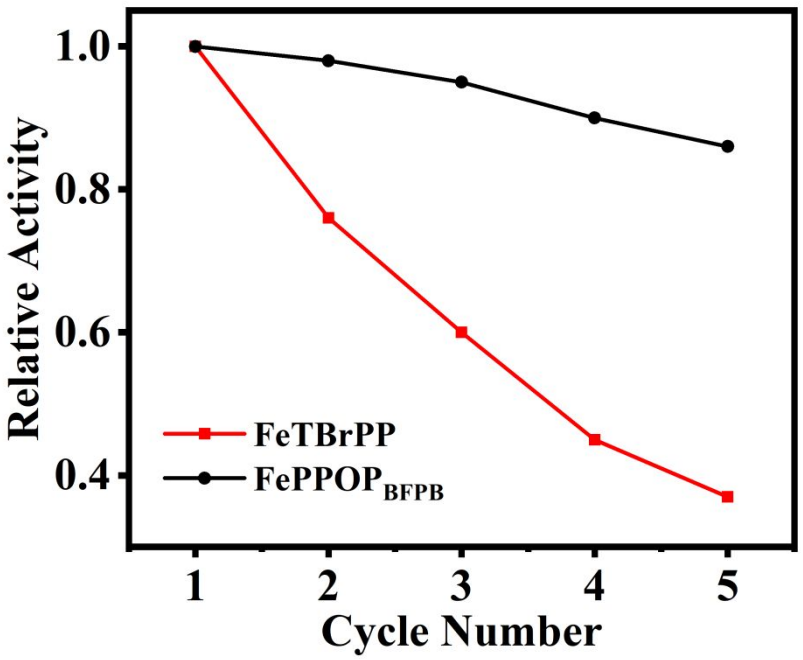

Figure S5. Recycled use of $FePPOP_{BFPB}$ and a normal iron porphyrin monomer [iron 5,10,15,20-tetrakis-(4'-bromoph-enyl)porphyrin, FeTBrPP] for catalyzed oxidation of TMB.

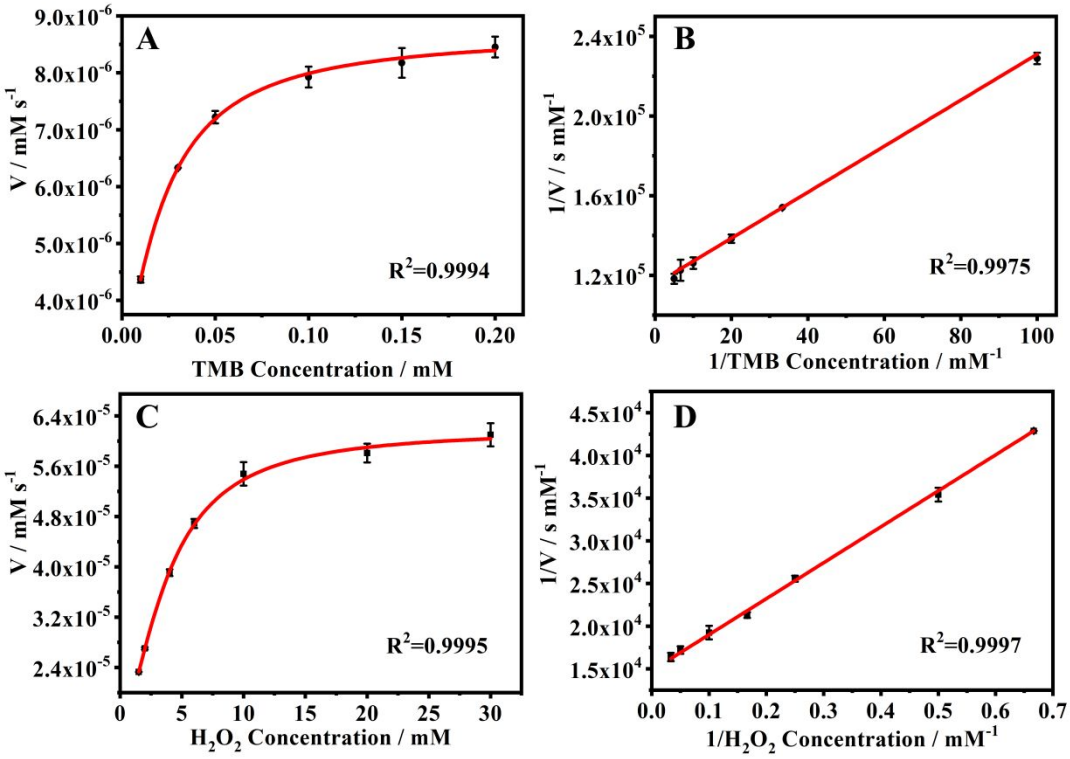

Figure S6. Steady-state kinetic assays of $FePPOP_{BFPB}$ using the Michaelis-Menten model (A, C) and the Lineweaver-Burk double-reciprocal model (B, D). The experiment was carried out in a reaction volume of 2 mL HAc-NaAc buffer solution (pH=3.8) in the presence of 10 μg·mL^{-1} of $FePPOP_{BFPB}$ at room temperature (25 °C). The concentration of H_2O_2 was fixed at 40 mM with various concentrations of TMB (A and B). The concentration of TMB was fixed at 0.1 mM with various concentrations of H_2O_2 substrate (C and D).

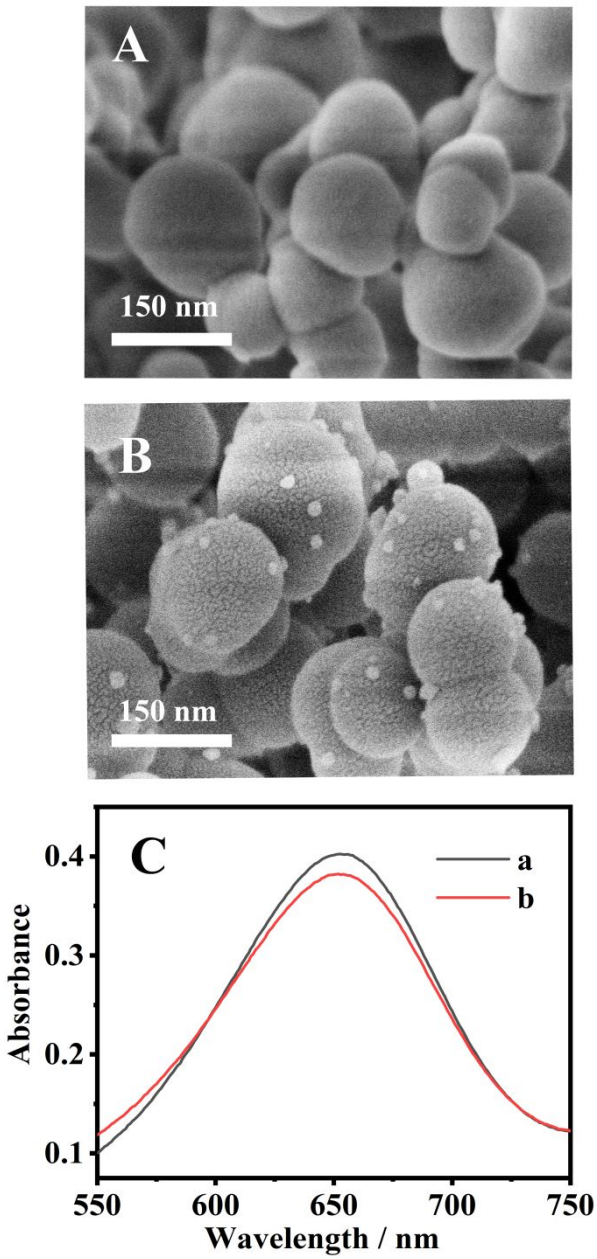

Figure S7. Comparison of the morphology characterization of (A) $FePPOP_{BFPB}$ and (B) Au@ $FePPOP_{BFPB}$. (C) Comparison of the catalytic activity of (a) $FePPOP_{BFPB}$ and (b) Au@ $FePPOP_{BFPB}$.

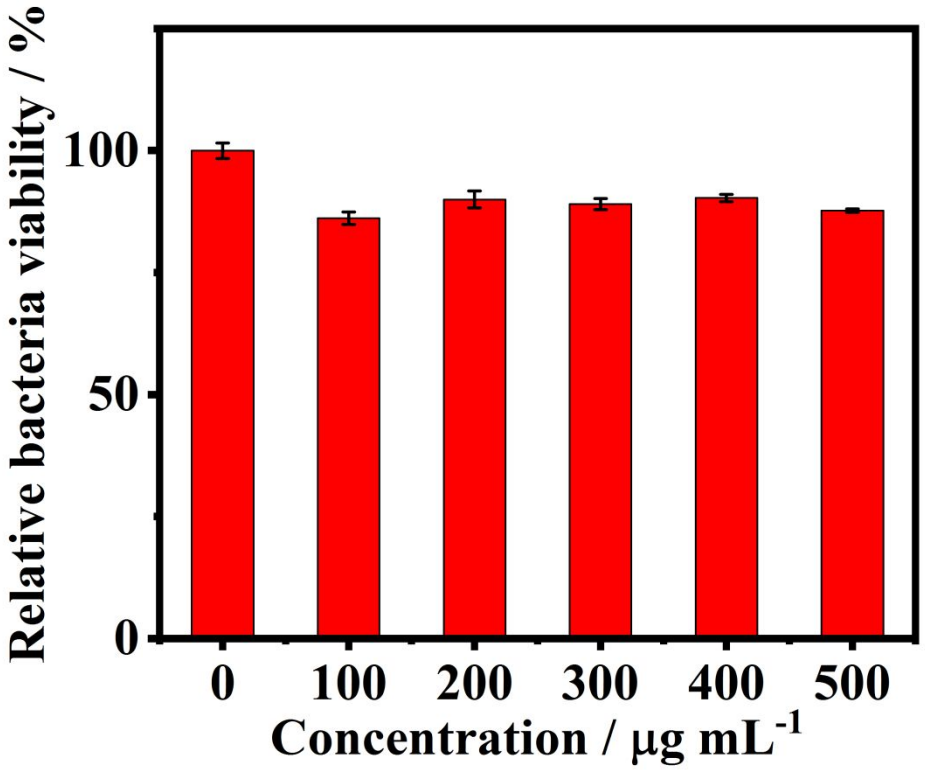

Figure S8. Cytotoxicity studies of the $FePPOP_{BFPB}$ on *S.aureus*.

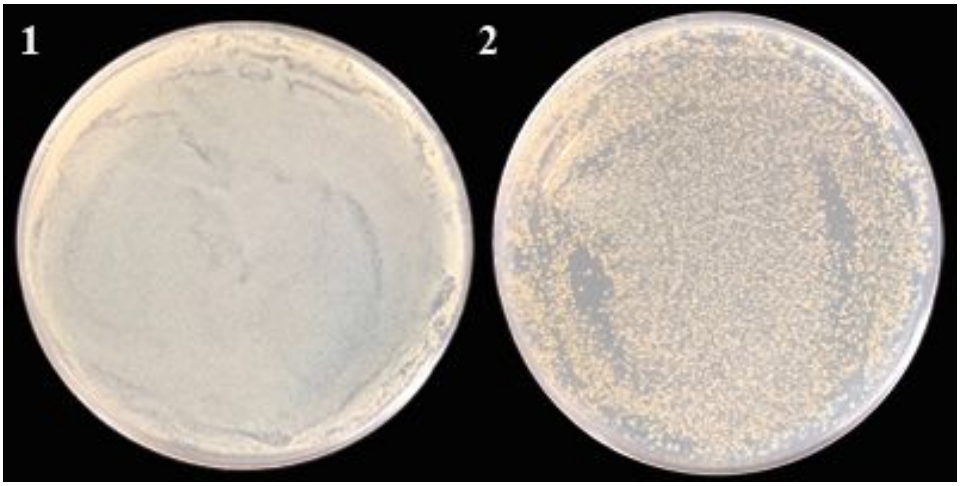

Figure S9. The photos of two plates seeded with 10^5 CFU/mL of *S. aureus* incubated in PBS at (1) 37 ^oC and (2) 52.5 ^oC for 20 min and cultured at 37 ^oC for 12 h.

Table S1. Comparison of the kinetic parameters of $FePPOP_{BFPB}$ with other catalysts. K_m is the Michaelis constant and V_{max} is the maximal reaction velocity.

Catalyst	K_m (mM)		V_{max} (mM/s)		Reference
	TMB	H_2O_2	TMB	H_2O_2	
$FePPOP_{BFPB}$	0.0099	2.81	8.62×10^{-6}	6.70×10^{-5}	This study
HRP	0.43	1.21	1.87×10^{-5}	5.88×10^{-5}	3
FePor-TFPA-COP	0.027	2.77	1.76×10^{-5}	8.33×10^{-4}	3
GO-Fe_3O_4	0.71	0.43	5.31×10^{-5}	1.31×10^{-4}	4
Hemin	4.84	2.74	4.69×10^{-5}	3.53×10^{-5}	5
H_2TCPP-ZnS	5.486	17.24	4.8×10^{-5}	1.0×10^{-4}	6

Table S2. Comparison of the current approach and relevant methods for analysis of pathogenic bacteria.

target bacteria	detection method	LOD (CFU/mL)	Reference
Listeria monocytogenes	PCR	30	7
S. aureus	FCM	33	8
S. aureus	FCM	10^2	9
S. aureus	CM	1.5×10^3	10
S. aureus	CM	4×10^3	11
S. aureus	FLS	2.9×10^2	12
S. aureus	ELISA	24	This study

Reference

(1) Shu, J.; Qiu, Z.; Zhuang, J.; Xu, M.; Tan, D. In Situ Generation of Electron Donor to Assist Signal Amplification on Porphyrin-Sensitized Titanium Dioxide Nanostructures for Ultrasensitive Photoelectrochemical Immunoassay. *ACS Appl. Mater. Interfaces* **2015**, *7*, 23812-23818.

(2) Zhang, X.; Gong, S.; Zhang, Y.; Yang, T.; Wang, C.; Gu, N. Prussian Blue Modified Iron Oxide Magnetic Nanoparticles and their High Peroxidase-Like Activity. *J. Mater. Chem.* **2010**, *20*, 5110.

(3) Deng, X.; Fang, Y.; Lin, S.; Cheng, Q.; Liu, Q.; Zhang, X. Porphyrin-Based Porous Organic Frameworks as a Biomimetic Catalyst for Highly Efficient Colorimetric Immunoassay. *ACS Appl. Mater. Interfaces* **2017**, *9*, 3514-3523.

(4) Dong, Y. L.; Zhang, H. G.; Rahman, Z. U.; Su, L.; Chen, X. J.; Hu, J.; Chen, X. G. Graphene Oxide-Fe_3O_4 Magnetic Nanocomposites with Peroxidase-Like Activity for Colorimetric Detection of Glucose. *Nanoscale* **2012**, *4*, 3969-76.

(5) Guo, Y. J; Deng, L; Li, J; Guo, S. J; Wang, E. K; Dong, S. J. Hemin-Graphene Hybrid Nanosheets with Intrinsic Peroxidase-Like Activity for Label-Free Colorimetric Detection of Single-Nucleotide Polymorphism. *ACS Nano* **2011**,5, 1282-1290.

(6) Liu, Q.; Chen, P.; Xu, Z.; Chen, M.; Ding, Y.; Yue, K.; Xu, J. A Facile Strategy to Prepare Porphyrin Functionalized ZnS Nanoparticles and their Peroxidase-Like Catalytic Activity for Colorimetric Sensor of Hydrogen Peroxide and Glucose. *Sensors and Actuators B: Chemical* **2017**, *251*, 339-348.

(7) Meng, X.; Li, F.; Li, F.; Xiong, Y.; Xu, H. Vancomycin Modified Pegylated-Magnetic Nanoparticles Combined with PCR for Efficient Enrichment and Detection of Listeria Monocytogenes. *Sensors and Actuators B: Chemical* **2017**, *247*, 546-555.

(8) Meng, X.; Yang, G.; Li, F.; Liang, T.; Lai, W.; Xu, H. Sensitive Detection of *Staphylococcus aureus* with Vancomycin-Conjugated Magnetic Beads as Enrichment Carriers Combined with Flow Cytometry. *ACS Appl. Mater. Interfaces* **2017**, *9*, 21464-21472.

(9) Shylaja, R.; Bhairab, M.; Padma, S.; Bhavanashri, N.; Joseph, K. Capture and Detection of *Staphylococcus aureus* with Dual Labeled Aptamers to Cell Surface Components. *International Journal of Food Microbiology* **2018**, *265,* 74-83.

(10) Sung, Y. J.; Suk, H. J.; Sung, H. Y.; Li, T.; Poo, H.; Kim, M. G. Novel Antibody/Gold Nanoparticle/Magnetic Nanoparticle Nanocomposites for Immunomagnetic Separation and Rapid Colorimetric Detection of *Staphylococcus aureus* in Milk. *Biosens.Bioelectron.* **2013**, *43*, 432-439.

(11) Yu, J.; Zhang, Y.; Zhang, Y.; Li, H.; Yang, H.; Wei, H. Sensitive and Rapid Detection of *Staphylococcus aureus* in Milk via Cell Binding Domain of Lysin. *Biosens. Bioelectron.* **2016**, *77*, 366-371.

(12) Kong, W.; Xiong, J.; Yue, H.; Fu, Z., Sandwich Fluorimetric Method for Specific Detection of *S. aureus* Based on Antibiotic-Affinity Strategy. *Anal. Chem*. **2015**, *87*, 9864-9868.